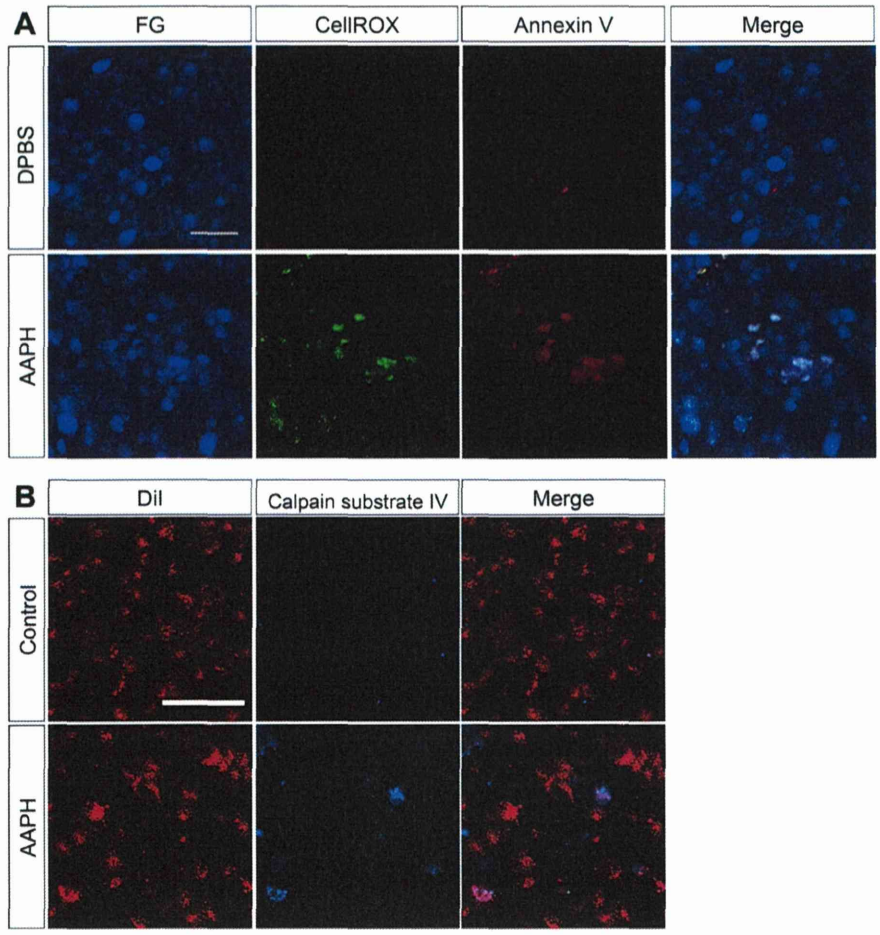

Fig. 2. Oxidative stress, calpain activation and apoptosis 24 h after AAPH administration. (A) Representative images of flat-mounted retinas showing CellROX and Annexin V signals, used to detect oxidative stress and apoptosis in the RGCs. CellROX and Annexin V signals were co-localized in the AAPH-treated retinas, while the DPBS-treated retinas showed no CellROX or Annexin V signals. (B) Representative appearance of DiI-labeled RGCs in flat-mounted retinas, with calpain substrate IV signals showing calpain activation. Twenty-four hours after AAPH administration, the control retinas showed no calpain substrate IV signals, while the AAPH-treated retinas showed co-localized calpain substrate IV signals and DiI-labeled RGCs. Scale bar: 50 μm.

Previous studies have reported that mitochondrial-derived death signaling is a major pathway of axonal damage-induced RGC death [21,22]. Mitochondria play an important role in the regulation of cell viability [23]. Oxidative stress induces mitochondrial-derived reactive oxygen species (ROS) generation and disturbs the function of calcium buffering [24–26]. To explore the mechanism of RGC death in the current investigation, we therefore assessed CellROX and Annexin V-positive RGCs in the AAPH-treated retinas, and obtained results suggesting that apoptosis of the RGCs was induced by ROS.

ROS induce the processing of mitochondrial apoptosis-inducing factor (AIF) and increase sensitivity to mitochondrial calpain, resulting in AIF cleavage and apoptosis [27]. Using immunoblotting, we investigated the AAPH-induced activation of calpain by testing for cleaved α-fodrin. Our results indicated that AAPH treatment induced fragmentation of α-fodrin as a result of calpain activation in the overall retina. Moreover, the co-localization of calpain substrate IV signals, which represent calpain activation, and DiI-labeled RGCs confirmed that calpain was activated in the RGCs. This suggests that the calpain pathway may be activated by an increased inflow of Ca^{2+} through Ca^{2+} channels under pathological conditions such as oxidative stress. Moreover, previous studies have shown that oxidative stress increases intracellular free Ca^{2+} levels, and activates Ca^{2+}-dependent enzymes [27–29]. These data suggest that oxidative stress and dysfunctional calcium buffering in the mitochondria may be major links with calpain activation in the retina, a finding that is consistent with our results.

Additionally, SNJ-1945 administration demonstrated a potent neuroprotective effect against AAPH-induced RGC death. Indeed, the number of RGCs after AAPH administration in the mice that received SNJ-1945 remained stable, in contrast with the mice that underwent the administration of AAPH and vehicle. SNJ-1945 reduced calpain activation and led to reduced cleaved α-fodrin intensity 24 h after AAPH administration. This result is consistent with past reports showing that oxidative stress caused calpain activation in RGCs that had been isolated *in vitro* [30] and that SNJ-1945 had a neuroprotective effect in the RGCs [7,31]. Here, using our *in vivo* model, we showed that the activation of calpain occurs downstream of oxidative stress, and that the inhibition of calpain activation was an effective way of preventing oxidative stress-induced RGC damage.

The animal model of oxidative stress described here may be appropriate for some purposes, such as investigating drug effects in cells that are sensitive to oxidative stress, but for other purposes, the intensity of AAPH-induced damage may be insufficient. Opportunities to refine this animal model therefore include the use of other ROS generators, such as rotenone [32] and paraquat, which

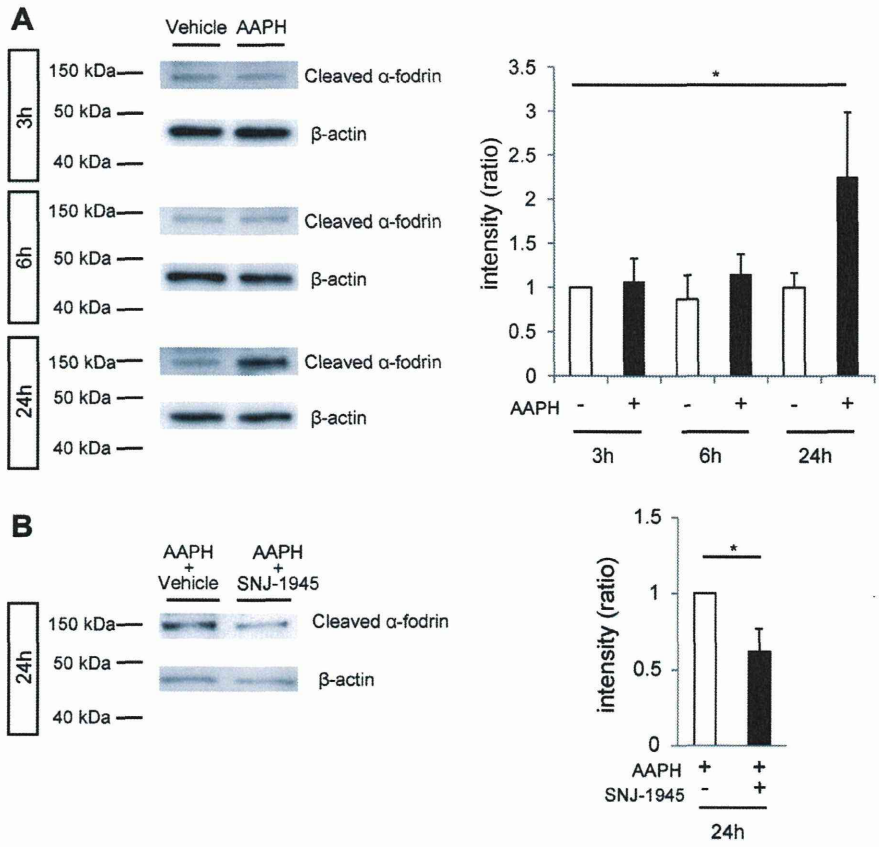

Fig. 3. Immunoblot analysis of calpain activation in mouse retinas after AAPH treatment. (A) Representative immunoblots and bar graphs showing the expression level of cleaved α-fodrin at each time point, compared with cleaved α-fodrin expression after 3 h in vehicle-treated retinas. β-Actin was used as an internal standard for the assessment of α-fodrin. The intensity of cleaved α-fodrin, i.e., of the 145-kDa fragments produced by activated calpain, was significantly higher 24 h after AAPH administration than after vehicle. Error bar: standard deviation ANOVA with Dunnett's post hoc analysis; $^*P < 0.05$. (B) Representative immunoblots showing calpain activation 24 h after AAPH administration, with or without SNJ-1945. The bar graphs show the expression level of cleaved α-fodrin in the SNJ-1945-treated and -untreated retinas. These results show that SNJ-1945 attenuated the intensity of α-fodrin cleavage. Error bar: standard deviation; *t*-test, $^*P < 0.05$.

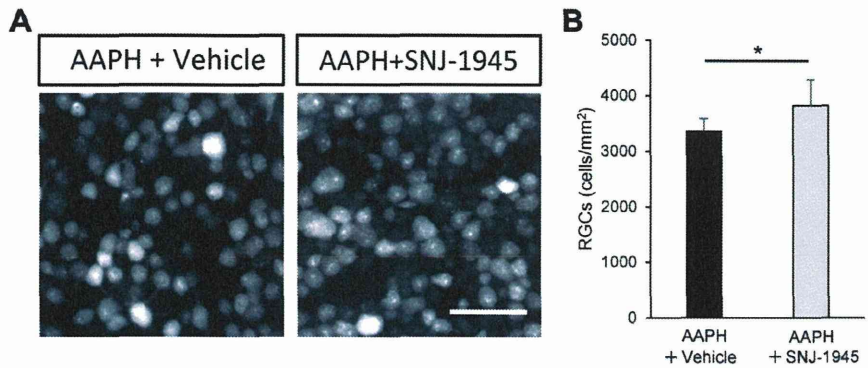

Fig. 4. Comparison of RGC density with and without SNJ-1945. (A) Representative appearance of RGCs in flat-mounted retinas 7 days after the intravitreal administration of AAPH. (B) Comparison of RGC density, determined by RGC counting, with and without SNJ-1945. RGC density was significantly higher with SNJ-1945, suggesting that SNJ-1945 protected the RGCs from AAPH-induced damage. Scale bar: 50 μm. Error bar: standard deviation; *t*-test, $^*P < 0.05$.

have a cytotoxic effect in retinal cells and dopaminergic cells [33,34].

In conclusion, we successfully established an *in vivo* model of oxidative stress in the RGCs with AAPH, and used this model to demonstrate that the calpain pathway is activated downstream of oxidative stress. Furthermore, suppressing calpain activation reduced RGC death in our model, suggesting that it may be a good candidate for neuroprotection therapy. Our findings may also be useful in future investigations of oxidative stress-related ocular diseases, such as glaucoma and diabetic axonal atrophy.

Acknowledgments

We thank Ms. Kaori Hanekawa for technical assistance and Mr. Tim Hilts for editing this document. We also thank Senju Pharmaceutical Co., Ltd. for the generous gift of SNJ-1945.

References

[1] J. Lee, M. Kannagi, R.J. Ferrante, N.W. Kowall, H. Ryu, Activation of Ets-2 by oxidative stress induces Bcl-xL expression and accounts for glial survival in amyotrophic lateral sclerosis, FASEB J. 23 (2009) 1739–1749.

[2] M. Ramamoorthy, P. Sykora, M. Scheibye-Knudsen, C. Dunn, C. Kasmer, Y. Zhang, K.G. Becker, D.L. Croteau, V.A. Bohr, Sporadic Alzheimer disease fibroblasts display an oxidative stress phenotype, Free Radic. Biol. Med. 53 (2012) 1371–1380.

[3] D.H. Choi, A.C. Cristovao, S. Guhathakurta, J. Lee, T.H. Joh, M.F. Beal, Y.S. Kim, NADPH oxidase 1-mediated oxidative stress leads to dopamine neuron death in Parkinson's disease, Antioxid. Redox Signal. 16 (2012) 1033–1045.

[4] K.N. Engin, B. Yemisci, U. Yigit, A. Agachan, C. Coskun, Variability of serum oxidative stress biomarkers relative to biochemical data and clinical parameters of glaucoma patients, Mol. Vis. 16 (2010) 1260–1271.

[5] A. Izzotti, A. Bagnis, S.C. Sacca, The role of oxidative stress in glaucoma, Mutat. Res. 612 (2006) 105–114.

[6] N. Himori, K. Yamamoto, K. Maruyama, M. Ryu, K. Taguchi, M. Yamamoto, T. Nakazawa, Critical role of Nrf2 in oxidative stress-induced retinal ganglion cell death, J. Neurochem. 127 (2013) 669–680.

[7] M. Ryu, M. Yasuda, D. Shi, A.Y. Shanab, R. Watanabe, N. Himori, K. Omodaka, Y. Yokoyama, J. Takano, T. Saido, T. Nakazawa, Critical role of calpain in axonal damage-induced retinal ganglion cell death, J. Neurosci. Res. 90 (2012) 802–815.

[8] C.Y. Wang, J.W. Xie, T. Wang, Y. Xu, J.H. Cai, X. Wang, B.L. Zhao, L. An, Z.Y. Wang, Hypoxia-triggered m-calpain activation evokes endoplasmic reticulum stress and neuropathogenesis in a transgenic mouse model of Alzheimer's disease, CNS Neurosci. Ther. (2013).

[9] T. Nakazawa, M. Shimura, R. Mourin, M. Kondo, S. Yokokura, T.C. Saido, K. Nishida, S. Endo, Calpain-mediated degradation of G-substrate plays a critical role in retinal excitotoxicity for amacrine cells, J. Neurosci. Res. 87 (2009) 1412–1423.

[10] A. Camins, E. Verdaguer, J. Folch, M. Pallas, Involvement of calpain activation in neurodegenerative processes, CNS Drug Rev. 12 (2006) 135–148.

[11] R. Piga, Y. Saito, Y. Yoshida, E. Niki, Cytotoxic effects of various stressors on PC12 cells: involvement of oxidative stress and effect of antioxidants, Neurotoxicology 28 (2007) 67–75.

[12] T. Nakazawa, M. Shimura, S. Endo, H. Takahashi, N. Mori, M. Tamai, N-methyl-D-aspartic acid suppresses Akt activity through protein phosphatase in retinal ganglion cells, Mol. Vis. 11 (2005) 1173–1182.

[13] T. Nakazawa, M. Shimura, M. Ryu, K. Nishida, G. Pages, J. Pouyssegur, S. Endo, ERK1 plays a critical protective role against N-methyl-D-aspartate-induced retinal injury, J. Neurosci. Res. 86 (2008) 136–144.

[14] T. Nakazawa, M. Takeda, G.P. Lewis, K.S. Cho, J. Jiao, U. Wilhelmsson, S.K. Fisher, M. Pekny, D.F. Chen, J.W. Miller, Attenuated glial reactions and photoreceptor degeneration after retinal detachment in mice deficient in glial fibrillary acidic protein and vimentin, Invest. Ophthalmol. Vis. Sci. 48 (2007) 2760–2768.

[15] Z. Banoczi, A. Alexa, A. Farkas, P. Friedrich, F. Hudecz, Novel cell-penetrating calpain substrate, Bioconjug. Chem. 19 (2008) 1375–1381.

[16] S.A. Keys, E. Boley, W.F. Zimmerman, A model membrane system to investigate antioxidants in bovine rod outer segments, Exp. Eye Res. 64 (1997) 313–321.

[17] S.A. Keys, W.F. Zimmerman, Antioxidant activity of retinol, glutathione, and taurine in bovine photoreceptor cell membranes, Exp. Eye Res. 68 (1999) 693–702.

[18] Z.K. Yu, Y.N. Chen, M. Aihara, W. Mao, S. Uchida, M. Araie, Effects of beta-adrenergic receptor antagonists on oxidative stress in purified rat retinal ganglion cells, Mol. Vis. 13 (2007) 833–839.

[19] P. Maher, A. Hanneken, The molecular basis of oxidative stress-induced cell death in an immortalized retinal ganglion cell line, Invest. Ophthalmol. Vis. Sci. 46 (2005) 749–757.

[20] N. Himori, K. Yamamoto, K. Maruyama, M. Ryu, K. Taguchi, M. Yamamoto, T. Nakazawa, Critical role of Nrf2 in oxidative stress-induced retinal ganglion cell death, J. Neurochem. (2013).

[21] S. Chierzi, E. Strettoi, M.C. Cenni, L. Maffei, Optic nerve crush: axonal responses in wild-type and bcl-2 transgenic mice, J. Neurosci. 19 (1999) 8367–8376.

[22] X. Qi, A.S. Lewin, L. Sun, W.W. Hauswirth, J. Guy, Suppression of mitochondrial oxidative stress provides long-term neuroprotection in experimental optic neuritis, Invest. Ophthalmol. Vis. Sci. 48 (2007) 681–691.

[23] R.L. Jayaraj, K. Tamilselvam, T. Manivasagam, N. Elangovan, Neuroprotective effect of CNB-001, a novel pyrazole derivative of curcumin on biochemical and apoptotic markers against rotenone-induced SK-N-SH cellular model of Parkinson's disease, J. Mol. Neurosci. (2013).

[24] I.J. Reynolds, T.G. Hastings, Glutamate induces the production of reactive oxygen species in cultured forebrain neurons following NMDA receptor activation, J. Neurosci. 15 (1995) 3318–3327.

[25] S.C. Chattipakorn, S. Thummasorn, J. Sanit, N. Chattipakorn, Phosphodiesterase-3 inhibitor (cilostazol) attenuates oxidative stress-induced mitochondrial dysfunction in the heart, J. Geriatr. Cardiol. 11 (2014) 151–157.

[26] I.B. Zavodnik, I.K. Dremza, V.T. Cheshchevik, E.A. Lapshina, M. Zamaraewa, Oxidative damage of rat liver mitochondria during exposure to t-butyl hydroperoxide. Role of Ca(2)(+) ions in oxidative processes, Life Sci. 92 (2013) 1110–1117.

[27] E. Norberg, V. Gogvadze, H. Vakifahmetoglu, S. Orrenius, B. Zhivotovsky, Oxidative modification sensitizes mitochondrial apoptosis-inducing factor to calpain-mediated processing, Free Radic. Biol. Med. 48 (2010) 791–797.

[28] S.K. Ray, M. Fidan, M.W. Nowak, G.G. Wilford, E.L. Hogan, N.L. Banik, Oxidative stress and Ca^{2+} influx upregulate calpain and induce apoptosis in PC12 cells, Brain Res. 852 (2000) 326–334.

[29] M. Azuma, T.R. Shearer, The role of calcium-activated protease calpain in experimental retinal pathology, Surv. Ophthalmol. 53 (2008) 150–163.

[30] M. Nakayama, M. Aihara, Y.N. Chen, M. Araie, K. Tomita-Yokotani, T. Iwashina, Neuroprotective effects of flavonoids on hypoxia-, glutamate-, and oxidative stress-induced retinal ganglion cell death, Mol. Vis. 17 (2011) 1784–1793.

[31] M. Shimazawa, S. Suemori, Y. Inokuchi, N. Matsunaga, Y. Nakajima, T. Oka, T. Yamamoto, H. Hara, A novel calpain inhibitor, {(1S)-1-({{(1S)-1-Benzyl-3-cyclopropylamino-2,3-di-oxopropyl)amino)carbonyl)-3-methylbutyl)carbamic acid 5-methoxy-3-oxapentyl ester (SNJ-1945), reduces murine retinal cell death in vitro and in vivo, J. Pharmacol. Exp. Ther. 332 (2010) 380–387.

[32] X. Zhang, D. Jones, F. Gonzalez-Lima, Mouse model of optic neuropathy caused by mitochondrial complex I dysfunction, Neurosci. Lett. 326 (2002) 97–100.

[33] H. Li, S. Wu, Z. Wang, W. Lin, C. Zhang, B. Huang, Neuroprotective effects of tert-butylhydroquinone on paraquat-induced dopaminergic cell degeneration in C57BL/6 mice and in PC12 cells, Arch. Toxicol. 86 (2012) 1729–1740.

[34] C.E. Abrahan, M.F. Insua, L.E. Politi, O.L. German, N.P. Rotstein, Oxidative stress promotes proliferation and dedifferentiation of retina glial cells in vitro, J. Neurosci. Res. 87 (2009) 964–977.

OPEN ACCESS Freely available online

PLOS ONE

RNA Sequence Reveals Mouse Retinal Transcriptome Changes Early after Axonal Injury

Masayuki Yasuda, Yuji Tanaka, Morin Ryu, Satoru Tsuda, Toru Nakazawa*

Department of Ophthalmology, Tohoku University Graduate School of Medicine, Sendai, Japan

Abstract

Glaucoma is an ocular disease characterized by progressive retinal ganglion cell (RGC) death caused by axonal injury. However, the underlying mechanisms involved in RGC death remain unclear. In this study, we investigated changes in the transcriptome profile following axonal injury in mice (C57BL/6) with RNA sequencing (RNA-seq) technology. The experiment group underwent an optic nerve crush (ONC) procedure to induce axonal injury in the right eye, and the control group underwent a sham procedure. Two days later, we extracted the retinas and performed RNA-seq and a pathway analysis. We identified 177 differentially expressed genes with RNA-seq, notably the endoplasmic reticulum (ER) stress-related genes *Atf3*, *Atf4*, *Atf5*, *Chac1*, *Chop*, *Egr1* and *Trb3*, which were significantly upregulated. The pathway analysis revealed that ATF4 was the most significant upstream regulator. The antioxidative response-related genes *Hmox1* and *Srxn1*, as well as the immune response-related genes *C1qa*, *C1qb* and *C1qc*, were also significantly upregulated. To our knowledge, this is the first reported RNA-seq investigation of the retinal transcriptome and molecular pathways in the early stages after axonal injury. Our results indicated that ER stress plays a key role under these conditions. Furthermore, the antioxidative defense and immune responses occurred concurrently in the early stages after axonal injury. We believe that our study will lead to a better understanding of and insight into the molecular mechanisms underlying RGC death after axonal injury.

Citation: Yasuda M, Tanaka Y, Ryu M, Tsuda S, Nakazawa T (2014) RNA Sequence Reveals Mouse Retinal Transcriptome Changes Early after Axonal Injury. PLoS ONE 9(3): e93258. doi:10.1371/journal.pone.0093258

Editor: Richard Libby, University of Rochester, United States of America

Received November 16, 2013; **Accepted** March 4, 2014; **Published** March 27, 2014

Funding: This study was supported in part by Grants-in-Aid from the Ministry of Education, Science and Technology of Japan (24659756 for T.N. and 40625513 for Y.T.) (http://www.mext.go.jp/english/). This study was also supported by JST Center for Revitalization Promotion (http://www.jst.go.jp/fukkou/), All Japan Coffee Association (http://coffee.ajca.or.jp/news/othernews/h26josei), Senju Pharmaceutical Co., Ltd. (http://www.senju.co.jp/) and NIDEK Co., Ltd. (http://www.nidek.co.jp/index-j.html). This study was also supported by the Great East Japan Earthquake Reconstruction Support project of the RIKEN Omics Science Center, the RIKEN Genome Analysis Service (GeNAS), Illumina Co. and CLC Bio Co. The funders had no role in study design, data collection and analysis, decision to publish, or preparation of the manuscript.

Competing Interests: This study was supported by donated funds from Senju Pharmaceutical Co., Ltd. and NIDEK Co., Ltd. This study was also supported by Illumina Co. and CLC Bio Co. as part of an Great East Japan Earthquake Reconstruction Support grant. This does not alter the authors' adherence to all the PLOS ONE policies on sharing data and materials.

* E-mail: ntoru@oph.med.tohoku.ac.jp

Introduction

Glaucoma is a leading cause of blindness worldwide [1]. It is characterized by glaucomatous optic neuropathy (GON), and is associated with optic nerve degeneration that results in progressive visual dysfunction [2]. In glaucoma patients, the number of retinal ganglion cells (RGCs) decreases due to axonal degeneration, resulting in visual dysfunction. Despite the attempts of many clinicians and scientists to identify the molecular mechanisms of pathogenesis in glaucoma, they are not yet well understood, possibly because of the multifactorial nature of glaucoma [3].

High intraocular pressure (IOP) is widely recognized as a major risk factor for glaucoma, and treatment to lower IOP is currently the only method that evidence has shown to prevent the progression of the disease [4]. Recently, many varieties of IOP-lowering eye drops have become clinically available to treat glaucoma. However, substantial reductions in IOP, up to 30%, fail to halt the progress of visual dysfunction in some patients, particularly those with normal tension glaucoma (NTG) [5]. In addition to IOP, risk factors for NTG include age, myopia [6], parapapillary atrophy (PPA) [7] and reduced ocular blood flow [8]. There is thus a necessity for further investigation of these IOP-independent mechanisms, and the development of new neuroprotective drug targets for glaucoma.

Many recent investigations have led to a growing understanding of the underlying mechanism of RGC death in glaucoma, which previous studies had found to be induced by axonal injury to the lamina cribrosa [3]. However, those studies were mainly designed around approaches that focused on only a few pathways [9,10]. In order to overcome the heterogeneous and multifactorial nature of glaucoma and find novel critical molecular targets for treatment, it is necessary to use a global approach (i.e., one including the transcriptome and proteome).

A simple animal model mimicking the pathogenesis of glaucoma is a useful tool in investigations of the mechanism of RGC death, because standard excisional biopsy is impossible in the case of the human retina [11]. In one of the most widely used models, optic nerve crush (ONC) is performed in mice to induce axonal injury, which is a contributor to the progression of RGC death in glaucoma [10,12–14]. Interestingly, in this model the number of RGCs is maintained for a short duration after ONC, and significant RGC loss is not observed until day 3 [10]. Significant axonal damage is known to occur in the retina before visual field defects become detectible [15]. It would therefore be very useful to develop diagnostic methods and drug targets that functioned in

these early stages of glaucoma. Analysis of post-ONC mouse retinas in the early stages of axonal injury, before RGC loss (i.e., on day 2), may give us valuable insights to help achieve this goal.

Microarray analysis is a common way to evaluate the expression level of large numbers of genes simultaneously. It has also been used to evaluate changes after axonal injury both in the retina in general and in isolated RGCs [16]. However, microarrays are only capable of measuring known transcripts, and do not allow the investigation of total genetic changes. By contrast, RNA sequencing (RNA-seq) is able to assess complete genes and splice variants, with a high degree of reproducibility that matches that of microarrays [17]. RNA-seq technology thus has the potential to give us very useful, detailed information on the mechanisms of disease, as well as unknown pathways and networks of disease, that may lead to the discovery of new treatment strategies.

The purpose of this study was thus to use RNA-seq to investigate the molecular mechanisms of damage in the early stages of the response to axonal injury, before the onset of RGC death. We believe that our study may open new avenues of investigation into treatment strategies for axonal damage associated with ocular diseases, especially glaucoma.

Results

RNA-seq analysis and global gene expression profiles in axonal injury

In order to investigate the transcriptome profile at an early stage after axonal injury, but before significant RGC loss [10], we performed an RNA-seq analysis of mouse retinas harvested 2 days after ONC or sham operations. In order to obtain triplicate results, three samples were obtained from each group, each sample being a combination of material from six unique retinas. Each of these samples was sequenced on one lane of the Illumina HiSeq2000 platform (Illumina, San Diego, CA). All sequence reads were mapped to the reference genome (NCBI37/mm9) with CLC Genomics Workbench (version 6.0.1) (CLC Bio, Aarhus, Denmark) [18,19]. The total number of reads per lane was approximately 400 million, and the total number of reads per sample ranged from 62.9 to 70.3 million. An average 73.8% of total reads were mapped in pairs to the reference genome (Table S1). Detailed mapping statistics are listed on Table S2. To determine the expression level of various genes and compare them between samples, we used variable RPKM (reads per kilobase of exon per million mapped reads) [20]. To examine the overall distribution of gene expression values, we created box plots of RPKM expression values with CLC Genomics Workbench (Figure 1A). Overall RPKM expression values were similar in each sample. We excluded genes that did not have a mean RPKM > 0.3 in at least one group, in order to remove background noise [21]. The number of genes with a mean RPKM > 0.3 in at least one group was 13160. These were used for the differential gene expression analysis [19]. Fold change (FC) differences between the mice that underwent ONC and those that underwent a sham operation were calculated. The Student's t-test was performed to compare the groups with R software (version 3.0.1) [22]. *P*-values were adjusted for multiplicity with the Bioconductor package qvalue to control the false discovery rate (FDR) [23]. Differentially expressed genes (DEGs) were defined as those with $|FC| > 1.5$ and FDR < 0.1 [24]. It is known that the cells affected by ONC are mainly RGCs. The abundance ratio of RGCs in retinal tissue has been reported to very low (less than 0.5%) [25]. Furthermore, an approximately 1.5 to 2-fold increase in gene expression (e.g., in *Jun, Jund and Gadd45a)* has been reported to be a significant change in a previous analysis of changes in the entire retina after optic nerve crush [26]. We therefore applied this relatively lower cutoff ($|FC| > 1.5$ and FDR < 0.1) in the current study. We created a volcano plot showing DEGs as red dots with the ggplot2 package in R software [27] (Figure 1B). We also conducted a hierarchical clustering analysis of DEGs from all samples with Ward's method of Euclidean distances [28], and created a heatmap with the heatmap.2 function of the gplots package of R software [29]. The results indicated that gene expression was similar in each group (Figure 1C).

Differentially expressed genes after ONC

The triplicate samples from the ONC and sham groups were assayed for DEGs, and 177 DEGs (132 up- and 45 downregulated genes) were identified (Table S3). The 10 most up- and downregulated genes are listed in Table 1. The expression changes of known RGC markers and axon regeneration markers [16,30,31] are summarized in Table 2. We found that the following RGC markers were significantly downregulated 2 days after ONC: *Nefh* (–2.24-fold), *Pou4f1* (–1.54-fold), *Pou4f2* (–2.40-fold), *Rbpms* (–1.62-fold) and *Sncg* (–1.77-fold). Interestingly, the expression of *Thy1* and *Pou4f3* did not change significantly at this time point (day 2). Generally, the expression of *Thy1* begins to decrease 3 days after axotomy in rats [32]. The following axon regeneration markers were significantly upregulated after ONC: *Gap43* (1.53-fold) and *Sprr1a* (23.81-fold).

A review of the published literature revealed that the following sets of endoplasmic reticulum (ER) stress-related genes have been shown to be significantly upregulated 2 days after ONC: *Atf3*, *Atf4*, *Atf5*, *Chac1*, *Ddit3*, *Egr1*, *Trib3* [33–35] (Table 2).

Significant networks and biological functions after ONC revealed by pathway analysis

To investigate the pathways involved in axonal injury, the DEG dataset was uploaded to Ingenuity Pathway Analysis (IPA, Ingenuity Systems, Redwood City, CA) and mapped to the Ingenuity Pathways Knowledge Base (IPKB) [36]. The 2 most significant networks are shown in Figure 2. Network 1 (Figure 2A) was associated with the "Cell Death and Survival", "Cancer" and "Cell Morphology" pathways. Network 2 (Figure 2B) was associated with the "Neurological Disease", "Nervous System Development and Function" and "Tissue Morphology" pathways. Table 3 lists the 5 most significant molecular and cellular functions. The most significant biofunction response, according to IPA, was for the "Cell Death and Survival" pathway, which involved 45 genes (Table S4).

RT-PCR validation of RNA-seq data

To validate the RNA-seq findings, we prepared new mouse retinas in each group, and performed RT-PCR on these new groups of retinas. We selected 14 genes (*Sprr1a, Mmp12, Sox11, Atf3, Tnfrsf12a, Hmox1, Plat, Egr1, Atf5, Ddit3, Jun, Pou4f2, Nefh* and *Pou4f1*) involved in the "Cell Death and Survival" pathway, and examined changes in their expression with RT-PCR (Table 4). We found that results obtained with RT-PCR were similar to those obtained with RNA-seq.

Upstream analysis and global network interactions after axonal injury

In order to investigate molecular network interactions, IPA performed an upstream regulator analysis. Table 5 shows the transcription factors that IPA predicted to be upstream regulators. The most significant was ATF4, but TP53, nuclear factor (erythroid-derived 2)-like 2 (NFE2L2) and DNA-damage inducible

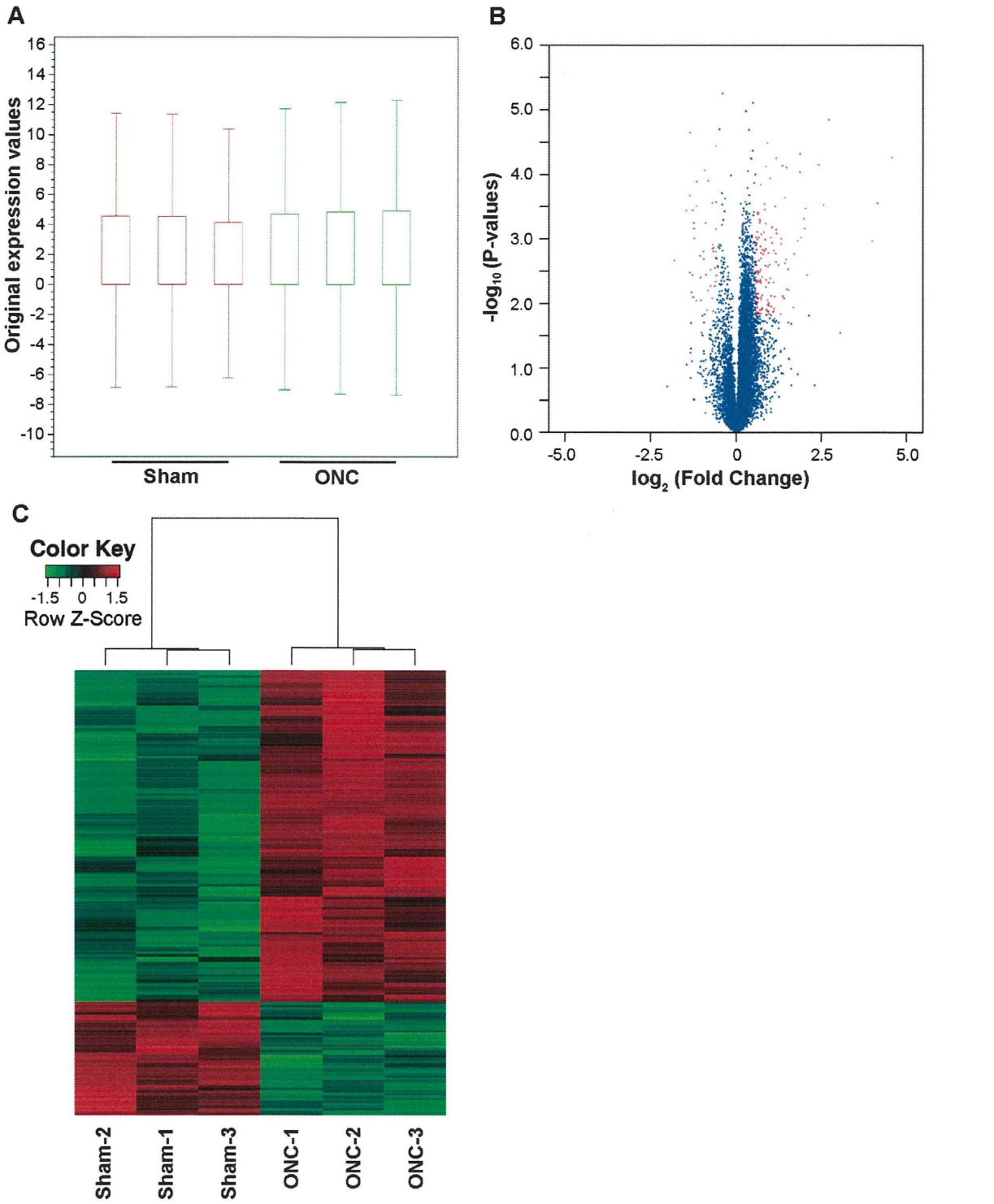

Figure 1. Gene expression profiles of the samples. (A) Box plot showing overall RPKM expression values for the ONC and control samples. (B) Volcano plot showing differentially expressed genes after axonal injury. For each plot, the X-axis represents $\log_2$ FC and the Y-axis represents $-\log_{10}$ (P-values). DEGs are shown as red dots. (C) Hierarchical clustering of DEGs after ONC. Red indicates increased expression and green indicates decreased expression. DEGs were defined as having absolute FC $>$ 1.5 and a FDR $<$ 0.1.
doi:10.1371/journal.pone.0093258.g001

Table 1. Top 10 upregulated and downregulated genes after ONC.

Symbol	Description	Gene accession	Fold change	*P*-value	FDR
Upregulated					
Sprr1a	Small proline-rich protein 1A	NM_009264	23.81	5.46E-05	0.026
Mmp12	Matrix metallopeptidase 12	NM_008605	17.82	2.80E-04	0.045
Ece1	Endothelin converting enzyme-like 1	NM_021306	15.96	1.08E-03	0.054
Chac1	ChaC, cation transport regulator-like 1 (E. coli)	NM_026929	6.61	1.44E-05	0.022
Sox11	SRY-box containing gene 11	NM_009234	5.92	2.98E-04	0.045
Atf3	Activating transcription factor 3	NM_007498	5.34	7.10E-05	0.028
Lgals3	Lectin, galactose binding, soluble 3	NM_001145953	4.23	3.66E-03	0.071
Phgdh	3-phosphoglycerate dehydrogenase	NM_016966	4.09	3.36E-04	0.045
Cdkn1a	Cyclin-dependent kinase inhibitor 1A (P21)	NM_007669	4.03	6.92E-04	0.051
Tnfrsf12a	Tumor necrosis factor receptor superfamily, member 12a	NM_013749	3.98	4.84E-04	0.048
Downregulated					
Gm6747	Predicted gene 6747	XM_003945591	−3.53	2.17E-03	0.061
Irx2	Iroquois related homeobox 2 (Drosophila)	NM_010574	−2.77	3.69E-04	0.045
Gm7244	Predicted gene 7244	NG_019018	−2.57	3.35E-03	0.069
Rasgrp2	RAS, guanyl releasing protein 2	NM_011242	−2.57	2.13E-04	0.043
Tppp3	Tubulin polymerization-promoting protein family member 3	NM_026481	−2.55	2.27E-05	0.022
Kcnd2	Potassium voltage-gated channel, Shal-related family, member 2	NM_019697	−2.47	6.78E-03	0.081
Opn3	Opsin 3	NM_010098	−2.44	3.63E-03	0.071
Ctxn3	Cortexin 3	NM_001134697	−2.42	3.62E-04	0.045
Pou4f2	POU domain, class 4, transcription factor 2	NM_138944	−2.40	7.99E-03	0.085
Pvalb	Parvalbumin	NM_013645	−2.37	5.66E-04	0.048

Differences were considered significant when FDR was < 0.1 and $|FC|$ was > 1.5.
doi:10.1371/journal.pone.0093258.t001

Table 2. Expression changes in genes associated with RGCs, axon regeneration and ER stress after ONC.

Symbol	Description	Gene accession	Fold change	*P*-value	FDR
RGC					
Nefh	Neurofilament, heavy polypeptide	NM_010904	−2.24	3.11E-04	0.045
Pou4f1	POU domain, class 4, transcription factor 1	NM_011143	−1.54	5.41E-03	0.077
Pou4f2	POU domain, class 4, transcription factor 2	NM_138944	−2.40	7.99E-03	0.085
Pou4f3	POU domain, class 4, transcription factor 3	NM_138945	1.04	NS	NS
Rbpms	RNA binding protein gene with multiple splicing	NM_019733	−1.62	1.43E-03	0.056
Sncg	Synuclein, gamma	NM_011430	−1.77	1.27E-04	0.032
Thy1	Thymus cell antigen 1, theta	NM_009382	−1.07	NS	NS
Axon regeneration					
Gap43	Growth associated protein 43	NM_008083	1.53	4.44E-03	0.073
Sprr1a	Small proline-rich protein 1A	NM_009264	23.81	5.46E-05	0.026
ER stress					
Atf3	Activating transcription factor 3	NM_007498	5.34	7.10E-05	0.028
Atf4	Activating transcription factor 4	NM_009716	1.61	5.65E-04	0.048
Atf5	Activating transcription factor 5	NM_030693	2.24	2.27E-03	0.062
Chac1	ChaC, cation transport regulator-like 1 (E. coli)	NM_026929	6.61	1.44E-05	0.022
Ddit3	DNA-damage inducible transcript 3	NM_007837	2.15	1.51E-03	0.056
Egr1	Early growth response 1	NM_007913	2.25	7.25E-04	0.051
Trib3	Tribbles homolog 3 (Drosophila)	NM_175093	2.89	2.98E-03	0.067

Differences were considered significant when FDR was < 0.1 and $|FC|$ was > 1.5. NS = not significant.
doi:10.1371/journal.pone.0093258.t002

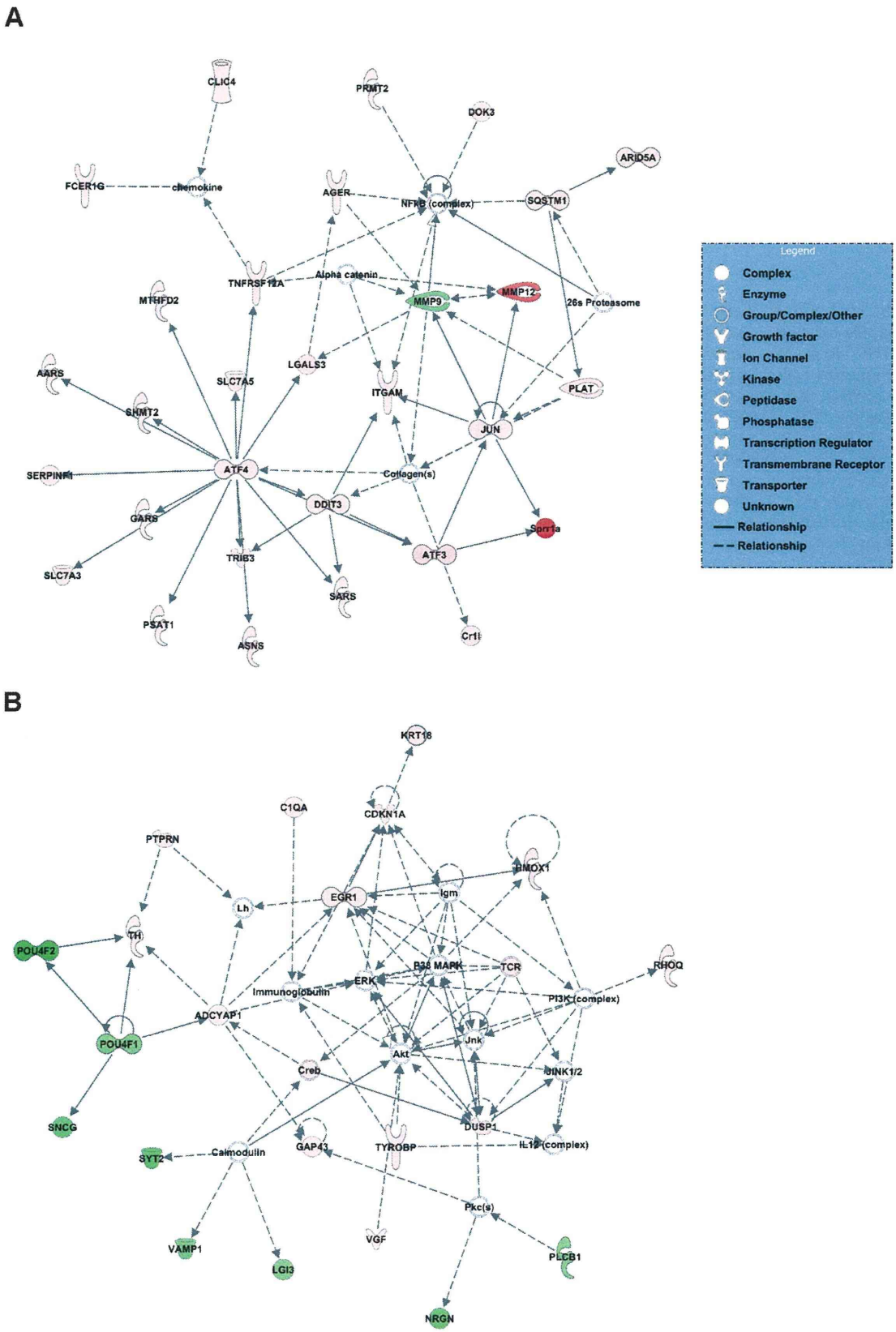
A
CLIC4
PRMT2
DOK3
ARID5A
FCER1G
chemokine
AGER
NFKB (complex)
SQSTM1
TNFRSF12A
Alpha catenin
MMP12
MMP9
26s Proteasome
MTHFD2
LGALS3
AARS
SLC7A5
ITGAM
PLAT
SHMT2
JUN
SERPINH1
ATF4
Collagen(s)
DDIT3
GARS
Sprr1a
ATF3
TRIB3
SLC7A3
SARS
PSAT1
ASNS
Cr1l
Legend
Complex
Enzyme
Group/Complex/Other
Growth factor
Ion Channel
Kinase
Peptidase
Phosphatase
Transcription Regulator
Transmembrane Receptor
Transporter
Unknown
Relationship
Relationship
B
KRT18
C1QA
CDKN1A
PTPRN
HMOX1
EGR1
Igm
Lh
TH
POU4F2
P38 MAPK
TCR
RHOQ
ERK
Immunoglobulin
PI3K (complex)
ADCYAP1
Jnk
POU4F1
Akt
Creb
SINK1/2
SNCG
DUSP1
GAP43
TYROBP
IL12 (complex)
SYT2
Calmodulin
Pkc(s)
VGF
VAMP1
PLCB1
LGI3
NRGN

Figure 2. Network analysis of the effect of ONC on gene expression. These post-ONC significance networks were generated by IPA. The 2 most significant networks are shown. (A) Network 1 was associated with the "Cell Death and Survival", "Cancer" and "Cell Morphology" pathways. (B) Network 2 was associated with the "Neurological Disease", "Nervous System Development and Function" and "Tissue Morphology" pathways. Red indicates upregulated genes, green indicates downregulated genes, and white indicates genes that were not annotated in this RNA-seq result but that formed part of the network.
doi:10.1371/journal.pone.0093258.g002

transcript 3 (DDIT3) were also determined to be upstream regulators activated after ONC. Data for ATF4, TP53, NFE2L2, DDIT3 and the target genes from the dataset were merged to create a graphical representation of the network of molecular relationships following ONC (Figure 3).

Discussion

In this study, we used RNA-seq to examine the global transcriptome profile early after axonal injury, before the onset of significant RGC death. We identified 177 DEGs including previously uninvestigated molecules in ONC. A pathway analysis of these DEGs revealed that the most significant biofunction in axonal injury was the "Cell Death and Survival" pathway. We found that the ATF4-regulated pathway and other sets of ER stress-related genes were significantly upregulated, and that NFE2L2 was also involved in axonal injury, as an upstream regulator. These results point to the critical role that ER stress plays in axonal damage-induced RGC death after ONC. Furthermore, the molecular mechanism of the response to axonal injury also involved antioxidative defense.

This study relied on an animal model of ocular disease in which axonal injury was induced by ONC [10]. Many animal models have been used in recent investigations of novel treatment strategies for glaucoma, such as neuroprotection. Various methods of inducing RGC loss in animals have previously been described, including ONC [10,14,37], optic nerve axotomy [32,38,39], intravitreal administration of N-methyl-d-aspartate [40–42] or Kainic acid [43–45] induction of glutamate excitotoxicity, and tumor necrosis factor-α-induced neuroinflammation [46,47]. In contrast to other models, ONC and optic nerve axotomy induce axonal damage by direct optic nerve injury, which is the main pathogenic component leading to RGC death in glaucoma [14]. In models using glutamate toxicity, RGC death occurs immediately with TUNEL signals detectible within 6 hours after injury [48,49]. On the other hand, in models using neuroinflammation, RGC death takes a few weeks and only a small number of cells are susceptible. Since the number of surviving RGCs did not significantly decrease until 3 days after ONC in mice [10], we were able to examine retinas on the second day after ONC and investigate the transcriptome profile of axonal injury-induced changes before the onset of RGC death. ONC was thus the most appropriate model of glaucoma for our study.

To our knowledge, this is the first report to use RNA-seq analysis to investigate the retinal transcriptome profile early after axonal injury. Although several researchers have conducted microarray analyses of axonal injury [16,50], the molecular mechanisms remain unclear. In contrast to RNA-seq, expression microarrays have a number of limitations (e.g., reliance on existing knowledge about the genome sequence, background noise and lower dynamic range). We therefore performed RNA-seq to generate a global view of the transcriptome after axonal injury.

Microarray analysis of rodent RGCs isolated with fluorescence-assisted cell sorting (FACS) has already been reported, and clarified the mechanism of axon regeneration after optic nerve axotomy [16]. Our RNA-seq analysis, by contrast, included cells from the entire retina. Since retinal glial cells are also affected by axonal damage after ONC [51], we therefore hypothesized that RNA-seq analysis of the entire retina would yield information that had not been revealed by previous microarray analyses of FACS-purified RGCs.

In axonal injury, RGCs decrease due to retrograde axonal degeneration [10]. Several RGC marker genes are known to be downregulated in response to axonal injury [30,52]. In the current study, *Pou4f1* (also known as Brn3a) and *Pou4f2* (also known as Brn3b) were downregulated 2 days after ONC (Table 2). Brn3 is a transcriptional factor expressed in the retina [53]. Furthermore, Brn3a is known to be a useful RGC marker, which can be used to identify and quantify RGCs both in controls and injured retinas [30]. In our study, *Thy1*, another well-known RGC marker [54], did not decrease significantly (Table 2). The loss of Brn3a-positive RGCs was detected earlier than the loss of Fluorogold-labeled RGCs [30]. *Brn3a* may therefore be a useful marker for evaluating RGC dysfunction in the early stages after ONC.

Axotomized RGCs are known to show many similar changes in gene expression during axon regeneration [55]. We found that *Sprr1a* and *Gap43*, genes that are related to axon regeneration, were significantly upregulated in the retina after axonal injury (Table 2). These results support previous findings obtained from a microarray analysis of FACS-purified RGCs taken from retinas subjected to axonal injury [16].

ER stress is thought to play an important role in the pathogenesis of several neurological disorders [56]. ER stress activates three unfolded protein pathways (UPRs) including RNA-dependent protein kinase (PKR)-like ER kinase (PERK), inositol-

Table 3. Top 5 molecular and cellular functions significantly modulated after ONC.

Category	*P*-value	Number of Molecules
Cell Death and Survival	7.45E-07-1.83E-02	45
Cellular Function and Maintenance	2.81E-06-1.83E-02	41
Cell-To-Cell Signaling and Interaction	4E-06-1.83E-02	40
Molecular Transport	5.13E-05-1.17E-02	42
Small Molecule Biochemistry	5.13E-05-1.83E-02	36

Significances were calculated with Fisher's exact test.
Differences were considered significant at the $P < 0.05$ level.
doi:10.1371/journal.pone.0093258.t003

requiring kinase 1 (IRE1) and ATF6. Prolonged ER stress can also induce apoptosis [35]. In the current study, the ER stress-related genes *Atf3*, *Atf4*, *Atf5*, *Chac1*, *Ddit3* (also known as C/EBP homologous protein (CHOP)), *Egr1* and *Trib3* were significantly upregulated 2 days after ONC (Table 2). Furthermore, IPA predicted that ATF4 was the most significant upstream regulator (Table 5). Under ER stress conditions, ATF4 is induced by eukaryotic inactivation factor 2α, downstream of the PERK pathway [57]. This suggests that ATF4 is the key upstream transcription factor induced by ER stress in the early stages of axonal injury.

IPA also predicted that CHOP was a significant upstream regulator (Table 5). CHOP is transactivated by ATF4, leading to ER stress-induced apoptosis [58]. Deletion of CHOP has been found to promote RGC survival [59]. According to IPA, ATF4 was an upstream regulator of CHOP (Table 5). This suggests that the ATF4-CHOP pathway plays an important role in axonal damage-induced RGC death. We also found that *Jun* was significantly upregulated (Table 4). JUN is known to be activated by the IRE1-JNK pathway under ER stress conditions [60], and can induce apoptosis [26]. Furthermore, we found that ER stress related-genes such as *Trib3* and *Chac1* were significantly upregulated after ONC (Table 2). TRIB3 has been reported to be involved in ER stress-induced apoptosis in 293 and Hela cells [35]. CHAC1 is involved in glutathione depletion and ROS generation [61] and is a proapoptotic component of the UPR, downstream of the ATF4-ATF3-CHOP cascade in primary human aortic endothelial cell lines [62]. To our knowledge, the role of TRIB3 and CHAC1 has not yet been investigated in the retina. The multiple ER stress-related pathways discussed above were activated concurrently in the retina after ONC. Therefore, a network-based approach [63], considering multiple pathways and molecules leading to cell death, is likely the best approach to treatment aimed at RGC protection after axonal injury, resembling the approach to photoreceptor protection that targets two cell death pathways [64].

Additionally, oxidative stress has been implicated in many neurodegenerative diseases [65,66]. In the current study, we found that the antioxidative response-related genes *Hmox1* and *Srxn1* were significantly upregulated 2 days after ONC (Table S3). IPA indicated that NFE2L2 was one of the upstream regulators activated after ONC, and that the increased expression of *Hmox1* and *Srxn1* was a downstream effect of NFE2L2 activation (Table 5 and Figure 3). NFE2L2, also known as Nrf2 (NF-E2 related factor 2), is a potent transcriptional activator and plays a central role in inducing the expression of many cytoprotective genes such as *Hmox1* and *Srxn1* [67,68]. Its translocation into the nucleus has been observed at an early stage after ONC [9]. This study also revealed that *Cdkn1a* (also known as p21) was significantly upregulated, and indicated that it interacts with Nrf2 (Figure 3). Cytoplasmic p21 has been reported to enhance axonal regeneration and functional recovery after spinal injury in rats [69]. Furthermore, it has been reported that transcriptional activation of cytoprotective genes by Nrf2 is potentiated in the presence of p21 through facilitated stabilization of Nrf2 [70]. In summary, the results of our study indicate that the Nrf2-related pathway is activated in response to axonal injury, which may be involved in a part of the defense mechanism suppressing RGC death and promoting axonal regeneration in the early stages of axonal injury. Enhancement of the antioxidant response, along with the inhibition of ER stress-related pathways (e.g., ATF-CHOP), may have a synergistic protective effect against RGC death after axonal injury.

The immune response has been reported to be involved in central nervous system (CNS) injury [55]. Our study found that *C1qa*, *C1qb* and *C1qc*, components of C1q belonging to the classical complement pathway, were significantly upregulated (Table S3). Furthermore, *C1qa* was included in the "Cell Death and Survival" pathway according to IPA (Table S4). C1q has been reported to be implicated in the pathogenesis of neurodegenerative diseases such as Alzheimer's disease [71]. A previous study used a microarray analysis to demonstrate that the complement pathway is upregulated in the retina 2 days after ONC [72], an observation

Table 4. RT-PCR validation of the expression of selected genes related to the "Cell Death and Survival" pathway.

Symbol	Description	Gene Accession	RNA-seq		RT-PCR	
			FC	*P*-value	FC	*P*-value
Sprr1a	Small proline-rich protein 1A	NM_009264	23.81	5.46E-05	232.12	2.79E-03
Mmp12	Matrix metallopeptidase 12	NM_008605	17.82	2.80E-04	84.75	2.27E-04
Sox11	SRY-box containing gene 11	NM_009234	5.92	2.98E-04	10.14	3.74E-04
Atf3	Activating transcription factor 3	NM_007498	5.34	7.10E-05	5.51	1.13E-02
Tnfrsf12a	Tumor necrosis factor receptor superfamily member 12a	NM_001161746	3.98	4.84E-04	7.57	1.27E-03
Hmox1	Heme oxygenase (decycling) 1	NM_010442	3.67	4.82E-05	4.50	1.53E-02
Plat	Plasminogen activator, tissue	NM_008872	2.26	5.63E-05	2.22	8.82E-03
Egr1	Early growth response 1	NM_007913	2.25	7.25E-04	4.21	2.15E-02
Atf5	Activating transcription factor 5	NM_030693	2.24	2.27E-03	2.82	5.50E-05
Ddit3	DNA-damage inducible transcript 3	NM_007837	2.15	1.51E-03	2.37	8.60E-06
Jun	Jun oncogene	NM_010591	2.00	1.14E-04	2.22	1.78E-03
Pou4f2	POU domain, class 4, transcription factor 2	NM_138944	−2.40	7.99E-03	−2.55	2.34E-06
Nefh	Neurofilament, heavy polypeptide	NM_010904	−2.24	3.11E-04	−2.36	3.58E-07
Pou4f1	POU domain, class 4, transcription factor 1	NM_011143	−1.54	5.41E-03	−2.25	1.55E-03

Differences between the NC and sham groups were analyzed with the t-test (RT-PCR: n = 6 for each group). Differences were considered significant at the $P<0.05$ level.
doi:10.1371/journal.pone.0093258.t004